# CDO Sensitivity Analysis for Robust Trajectory Planning under Uncertain Weather Prediction

Shumpei Kamo, Judith Rosenow, and Hartmut Fricke
Institute of Logistics and Aviation
Technische Universität Dresden
Hettnerstraße 1-3, 01062 Dresden, Germany
Email: Shumpei.Kamo@tu-dresden.de

***Abstract*—When planning and predicting a flight trajectory, uncertainties are inherent both in the current values of various influencing factors and in their evolution. These uncertainties can turn initially "optimized" trajectories into impossible or at least less attractive solutions later when it is executed. In order to support a more robust trajectory planning for Continuous Descent Operations (CDO), this paper investigates how variations of those influencing factors impact the trajectory optimization fidelity. For this purpose, a set of optimal trajectories are generated for each of the variations and their sensitivities are analyzed. The trajectory optimization is formalized as a multi-phase optimal control problem and is numerically solved with the Legendre-Gauss Pseudospectral Method (LGPM). An iterative process is proposed to determine the required number of collocation points to grant a pre-set level of convergence. Case studies are carried out for International Standard Atmosphere (ISA) baseline conditions as well as for wind and temperature variations as relevant representatives of the weather prediction uncertainties. The numerical simulation results show shifts from the reference trajectory depending on wind and temperature variation. Uncertain wind speed caused a larger solution space and more variation in fuel burn than temperature errors. The designed solution spaces, especially the earliest and latest ToD locations, give pilots and air traffic controllers a good reference where their aircraft is expected to match best CDO goals under the individually prevailing uncertainties. We believe that such additional flight envelope information should complement current vertical path displays in glass cockpits to foster robust flight planning and execution.**

***Keywords*—Continuous Descent Operations, Trajectory optimization, Expected solution space, Multi-phase optimal control**

## NOMENCLATURE

| | |
|---|---|
| $t$ | Time |
| $V$ | Airspeed |
| $s$ | Along-track distance |
| $h$ | Altitude |
| $m$ | Gross mass |
| $F_T$ | Thrust |
| $\gamma$ | Flight path angle |
| $\delta_{SB}$ | Speed brake |
| $\boldsymbol{x}$ | State vector |
| $\boldsymbol{u}$ | Control vector |
| $()_0$ | Initial value |
| $()_f$ | Final value |
| $()^{(c)}$ | Value in the cruise phase |
| $()^{(d)}$ | Value in the descent phase |
| $J$ | Objective functional |
| $T$ | Temperature |
| $L$ | Lift |
| $D$ | Drag |
| $C_D$ | Drag coefficient |
| $U_w$ | Longitudinal wind speed |
| $FC$ | Fuel consumption |
| $C_I$ | Cost index |
| $C_f$ | Fuel price per unit mass |
| $C_t$ | Time-related costs per unit flight time |
| $N$ | Number of collocation points |
| $N^*$ | Optimal number of collocation points |
| $N_k$ | Num. of collocation points in the $k$-th iteration |
| $\Delta N$ | Increment of $N$ between iterations |
| $\varepsilon$ | Tolerance of objective function for termination |
| $\varepsilon_t^{patient}$ | Time limit to judge the iteration converges |

## I. INTRODUCTION

Continuous Descent Operations (CDO) is a descent procedure that enables a flight profile with low thrust settings and a low drag configuration, taking the form of a continuously descending path with respect to the aerodynamic glide number, with a minimum of level flight segments [1]. CDO has potential to reduce fuel burn and noise during descent and has been tested at various airports worldwide [2], supported by variety of proposed methods for CDO trajectory optimization and prediction [3]–[6]. Ex-post analyses at airports offering CDO however show that the executed flight profiles were only rarely optimal and that relevant capacity shortages resulted [3]. This was mainly due to wrong assumptions, which then prevented Air Traffic COntrollers (ATCOs) from clearing and pilots from executing the optimized trajectory. It was further found, that different categories of uncertainties impact the trajectory prediction process, such as poorly predicted weather, flight performance modeling error or atypical human behavior. Dedicated efforts have been made to characterize these categories of uncertainty [7] and to find the best or robust trajectory [8] considering the whole possible scenarios.

Trajectory planning is usually carried out assuming certain reference conditions. These include available weather

978-1-7281-9825-5/20/$31.00 ©2020 IEEE

report, point mass dynamics representing the aircraft's performance [4], [5], [9] and no latency in human behavior. The gap between the reference and the "true" conditions that the aircraft will experience brings offsets from the initially calculated optimum. In an extreme situation, the difference might lead to an infeasible trajectory out of the prescribed flight envelope or a less optimal trajectory. The optimal trajectory under the true conditions can only be obtained by post-flight calculation when all the true conditions become known. When planning a CDO trajectory, it is thus helpful to create and know a so-called solution space for a given CDO that grants robustness against a minimum quality, which is made by accumulating optimized trajectories that correspond to each varied condition. With the solution space, ranging from the expected earliest to the latest Top of Descent (ToD), pilots and ATCOs can plan an alternative trajectory, preparing for the case where it is found inappropriate to follow the reference trajectory for any reason. Especially, investigation of the "second best" solution (or more generally speaking of a sub-optimal solution still satisfying a pre-set quality index) allows for quick and robust in-flight adaptations prior to reaching the ToD.

This paper calculates and discusses how altering environmental conditions can affect the optimized trajectory and the corresponding costs, taking weather deviation (wind and temperature) from the International Standard Atmosphere (ISA) into account as examples. Based on the analysis, the solution space is modeled. The trajectory optimization problem is formalized with optimal control to search the optimal way to control the dynamical system (aircraft) and is numerically solved using the pseudo-spectral method, which represents a trajectory with discrete variables.

## II. State of the Art

Benefits of CDO compared to the conventional step descent have been intensively evaluated in terms of fuel savings, emission and noise through simulation [10]–[12], data analysis [13], [14] as well as flight tests [15]. Despite these attractive benefits, CDO's limited predictability for ATCO makes it not easy to be implemented in the daily operations. Fricke et al. analyzed operational data and the optimal CDO trajectories [3] based on their detailed flight performance models and on ground-based flight performance charts [16]. They found that the analyzed flight did not necessarily adhere to the ICAO designed CDO corridor and that the poor execution of CDO was found to degrade its potential of fuel savings.

Variety of methods have been proposed and tested to optimize CDO trajectories and enhance the predictability. Park et al. focused on optimizing a vertical CDO trajectory to minimize flight time and fuel and compared the results to the reference VNAV CDO trajectory [4]. They also proposed a sub-optimal CDO trajectory to significantly reduce calculation time, which is one of the well-known pitfalls of optimal control [17]. De Jong proposed an operational procedure and trajectory re-planning strategy for CDO named Time and Energy Management Operations (TEMO) [5]. The concept aimed at finding an optimal trajectory in terms of kinetic and potential energy management, and also aimed at being robust under trajectory prediction errors. Performance of TEMO was further studied by Dalmau et al. [18] and it was found to be capable of dealing with required time of arrival (RTA) and wind uncertainty. Stell developed a method to accurately predict spatial location of ToD on a mathematical model basis [6]. Simplified flight dynamics were used and the location was predicted using polynomial approximation with different complexity levels. The model was compared with experimental flight data and the simple polynomial approximation was found to be sufficient.

Trajectory optimization is often formalized as an optimal control problem. Soler proposed a general framework for how to apply (multi-phase mixed-integer) optimal control to trajectory optimization and solved wide range of scenarios and problem settings [19]. González-Arribas et al. expanded the deterministic framework to stochastic optimization and proposed a robust trajectory planning algorithm, which tries to find the time series of control inputs to minimize overall possible situations. The enhanced system was tested in a scenario where weather prediction has uncertainties (e.g. on wind) [8]. Dalmau et al. optimized vertical trajectory for the entire flight and compared continuous operations to conventional procedures, both of which were formalized using multi-phase optimal control [9]. Park et al. [4], [17] and De Jong [5] also applied optimal control to do vertical trajectory planning.

Thanks to the intensive effort on optimizing and analyzing CDO trajectories, optimal CDO trajectory determination has become possible. However, application of optimal control to trajectory calculation is still limited to relatively simple formalizations that assume smoothness and weak non-linearity of their solution functions, since the problem becomes too complex to solve computationally otherwise. Solving an optimal control problem that is formalized more closely to practical operations and real flight performance is still challenging.

Another challenge is a variety of uncertainties that affect trajectory prediction. According to Casado et al., the major uncertainty sources include modeling errors, initial conditions, intent uncertainties, flight technical errors and weather forecasts [20]. Among them, weather forecast errors, as an external disturbance on an aircraft, have particular impact and especially wind, pressure and temperature errors affect along-track and vertical trajectory, which are crucial to to predict descent trajectory (Mondoloni [21]).

As one of the external disturbances, Park et al. put wind variation in optimal-control based CDO trajectory optimization and analyzed sensitivity of trajectory prediction to wind variation [4]. They reported variation of ToD location up to about 6 NM affected by head wind and tail wind up to 10 m/s (19.4 kt). De Jong evaluated their TEMO guidance strategy under wind estimation errors up to 5 kt and found achieved compensation of the effect [22]. Verhoeben et al. and Dalmau et al. did further studies that analyzed the effect of wind prediction error on TEMO constrained by RTA [18], [23].

Based on the literature review, CDO trajectory as an optimal descent was found to have been intensively studied and im-

plemented. However, relevant uncertainties have not so widely considered in optimal CDO trajectory planning. Especially the expected solution space, an area where the aircraft will be expected to fly considering the anticipated uncertainties, facilitates the CDO trajectory prediction for both pilots and ATCOs and it should be more deeply studied. This paper takes variations in weather prediction and evaluate how they affect the shape of the solution space and the key performance indices.

## III. Problem formalization

### A. Fundamental perspective for trajectory optimization

This section explains the fundamental viewpoint we have when we formalize the trajectory optimization problem based on the optimal control theory.

This study considers the flight state vector

$$\boldsymbol{x}(t) = \{V(t), s(t), h(t), m(t)\} \in \mathbb{R}^4 \tag{1}$$

containing airspeed $V$, along-track position $s$, altitude $h$ and total mass $m$, and the control input vector

$$\boldsymbol{u}(t) = \{F_T(t), \gamma(t), \delta_{SB}(t)\} \in \mathbb{R}^3 \tag{2}$$

containing thrust $F_T$, flight path angle $\gamma$ and speed brake $\delta_{SB}$, as fundamental variables describing an aircraft trajectory in 4D, and regards the trajectory optimization problem as a problem to determine these variables as functions of time, or time histories. All the other physical quantities are derived from the state and control variables as shown later in this section. In this paper, the term *variable* only refers to those forming the state and control vectors. The other static quantities, as specified in Section V-A, are called *parameters*. The following formalization is derived in terms of the state and control variables and the models are written as functions of these variables.

This study assumes the situation, where pilots intend to complete the cruise phase and to plan their CDO trajectory especially the ToD location. The flight trajectory that the aircraft has already experienced is fixed. Therefore the flight states at the moment of trajectory planning (the "current" moment) are also fixed and known. Theoretically, they are the initial conditions of our trajectory optimization problem. As the already fixed trajectory before the current state is out of interest for the study, the time and the along-track position are initialized at the moment ($t = 0, s = 0$). The final cruise segment is required to allow us to compare different profiles in terms of ToD location.

We build the trajectory down to the Final Approach Fix (FAF). This study assumes the FAF to be fixed and published (therefore pre-known). Consequently, the along-track position $s$ and altitude $h$ that the trajectory must satisfy when passing the FAF is assumed to be known. A descending aircraft is operationally required to reduce the airspeed along the segment (from fixed cruise Mach number typically down to minimum clean speed). The study sets the speed that the aircraft must meet at the FAF ($t = t_f$) to model this operational constraint. These are described as final conditions. The aircraft gross mass $m$ at FAF is however not previously known nor the state and control variables in between the initial and final moment. The summary of the above discussion is:

**Known:** $V, s, h, m$ at $t = 0$ and $V, s, h$ at $t = t_f$
**Unknown:** $m$ at $t = t_f$, $\boldsymbol{x}(t), \boldsymbol{u}(t)$ at $\forall t \in (0, t_f)$ and $t_f$

Consequently, we aim to determine the unknown time histories of the state and control variables, or in other words their mathematical representation as functions of time. The optimized function values at each $t$ are searched within reasonable boundaries called path constraints. A so called free-time fixed-endpoint optimal control problem [24] fits these problem settings, which aims by optimally transferring a dynamical system (aircraft states in this case) from the initial to a final condition, as shown below. In the following formalization, the international system of units (SI units) is assumed unless a specific unit is mentioned in the description.

### B. Flight dynamics (equations of motion)

The following longitudinal point mass equations of motion are used in this study, referring to an aerodynamic coordinate system for (3), respectively geodetic coordinates system (4) and (5) according to DIN 9300 or ISO 1151-2:1985.

$$m\dot{V} = F_T - mg\sin\gamma - D \tag{3}$$
$$\dot{s} = V\cos\gamma + U_w \tag{4}$$
$$\dot{h} = V\sin\gamma \tag{5}$$
$$\dot{m} = -FC \tag{6}$$

The aircraft is assumed to track a pre-defined horizontal path and thus horizontal movement is neglected. As change of the flight path angle is small ($\dot{\gamma} \approx 0$), vertical equilibrium ($L \approx mg$ in the vertical equation of motion $\dot{\gamma} = L - mg\cos\gamma$) is also assumed. In terms of wind, steady wind is assumed and thus the wind acceleration $\dot{U}_w$ in (3) is neglected. Positive $U_w$ refers to horizontal tail wind and negative sign means head wind. Mathematical derivation of the wind effect on the flight dynamics is discussed for example in [4].

Phase-specific assumptions are introduced as follows to characterize each flight phase.

**Cruise phase**

In the cruise phase, steady level flight, or constant airspeed and altitude, is assumed to model operational limitations. Aircraft are basically supposed to keep certain airspeed and altitude which are agreed between the pilots and ATCOs in order to keep required separation in traffic. These limitations are physically described by $\dot{V} = 0$ and $\dot{h} = 0$ and the latter leads to $\gamma = 0$ therefore $\sin\gamma = 0$ and $\cos\gamma = 1$. These assumption bring longitudinal balance thrust $F_T = D$. Therefore, $F_T$ and $\gamma$ are not needed to be searched in the optimization and $h$ is no longer dominated by the dynamics. That means the three variables and the corresponding dynamics (3) and (5) can be excluded from the optimization. Also, speed brake use is forbidden in this phase ($\delta_{SB} = 0$). As a result, the

state vector is simplified as $\boldsymbol{x}^{(c)} = \{s, m\} \in \mathbb{R}^2$, whereas the control vector has no component $\boldsymbol{u}^{(c)} = \mathbf{0}$. Although the control vector is a zero vector in this phase, the state vector still has components and their equations (4), (6) are one of the constraints in our trajectory optimization as we see at the end of this section. Therefore, the cruise phase, an interval between the aircraft's initial position and the ToD location, certainly affects optimization results.

**Descent phase**

Idle thrust descent is assumed in this study, which means thrust $F_T$ in (3) is always zero. Unlike the cruise phase, the flight path angle $\gamma$ is not restricted to a fixed value. The state and control vectors for the descent phase are therefore simplified as $\boldsymbol{x}^{(d)} = \{V, s, h, m\} \in \mathbb{R}^4$, $\boldsymbol{u}^{(d)} = \{\gamma, \delta_{SB}\} \in \mathbb{R}^2$.

### C. Flight performance model

Aircraft gross mass is modeled as a sum of operational empty weight $m_{oew}$, payload $m_p$ and fuel mass $m_f$ (all in [kg]).

$$m = m_{oew} + m_p + m_f \tag{7}$$

$m_{oew}$ and $m_p$ are assumed to be constant and thus $\dot{m} = \dot{m}_f$ in (6), i.e. the fuel consumption $FC$ in [kg/s].

In terms of drag coefficient and $FC$, models described in BADA4 [25] (direct thrust parameter input) are used. There, $FC$ is modeled as a non-linear function of thrust, Mach number, pressure and temperature. This study assumes international standard atmosphere (ISA), so speed of sound, pressure and temperature are known functions of altitude. Therefore, fuel consumption in this study is a function of airspeed $V$, altitude $h$ and thrust $F_T$. $FC$ is defined positive at all time.

$$FC(V, h, F_T) > 0 \tag{8}$$

Parasite drag is calculated through the drag coefficient $C_D$.

$$D\left(V,\, h,\, m_t,\, \delta_{SB}\right) = \frac{1}{2}\,\rho\, V^2\, S\, C_D \tag{9}$$

where $\rho$ and $S$ denote atmospheric pressure and the aircraft's reference wing area, respectively. $C_D$, as modeled in BADA4, consists of terms corresponding to clean and non-clean aircraft configurations. The clean drag coefficient is a function of lift coefficient $C_L$ and Mach number. Considering the assumption that the lift is balanced the weight, $C_D$ is a function of $V$, $h$ and $m_t$. Speed brake effect is considered as the non-clean drag configuration.

$$C_D(V, h, m_t, \delta_{SB}) = C_D^{clean} + 0.03\ \delta_{SB} \tag{10}$$

Important to note is that $\delta_{SB}$ is defined as a linear function between 0 and 1 though BADA4 only allows binary settings with $\delta_{SB}$ = 0 or 1. This linear interpolation is motivated to express intermediate level of speed brake deployment between none and fully deployed, as given for typical commercial aircraft such as the Airbus A320.

### D. Objective functional

The objective functional $J$ in [€] considers time and fuel costs, corresponding to the first and second terms of (11), respectively.

$$\begin{aligned} J\left(V,\, h,\, F_T;\, t_f^{(d)}\right) &= C_t t_f^{(d)} + C_f \int_{t_0^{(c)}}^{t_f^{(d)}} FC dt \\ &= C_f \left( C_I t_f^{(d)} + \int_0^{t_f^{(d)}} FC dt \right) \end{aligned} \tag{11}$$

Time costs are defined as the costs [€] charged for the flight time [s] of the considered flight phases from the aircraft's initial position to the target FAF, which is represented by $t_f^{(d)}$ in our formalization. Linear relationship is assumed between the time costs and $t_f^{(d)}$ through a coefficient $C_t$ [€/s]. The coefficient is modeled with so-called cost index $C_I$ [kg/s] implemented in current Flight Management Systems (FMS). By transforming its definition $C_I = \frac{C_t}{C_f}$, the coefficient is obtained as $C_t = C_f C_I$. As for the fuel costs, they are defined as costs [€] charged for the fuel burn [kg] in the considered flight phases. The costs are assumed to be proportional to the burned fuel and the coefficient $C_f$ is a fuel price [€/kg].

As we can see in the formalization, the time costs are directly dependent on the total flight time $t_f^{(d)}$ and the fuel costs on $V, h, F_T$ through $FC$. The variables are a part of the decision variables in our trajectory optimization. In this research, $C_I$ is set by the user when creating a scenario and is then kept constant for the scenario.

### E. Constraints

**Path constraints**

Since the order of the two phases that the descent phase comes after the cruise phase is fixed, the times at the phase edges have the following relationships:

$$t_0^{(c)} < t_f^{(c)} = t_0^{(d)} < t_f^{(d)} \tag{12}$$

Here, important note is that the final time at cruise and the initial time at descent $t_f^{(c)} = t_0^{(d)}$ are equivalent to the time at ToD.

Upper and lower limits for state and control variables are imposed to prevent the optimizer from searching in the outside the problem domain.

$$\boldsymbol{x}_{min}^{(phase)} \leq \boldsymbol{x}^{(phase)} \leq \boldsymbol{x}_{max}^{(phase)} \tag{13}$$

$$\boldsymbol{u}_{min}^{(phase)} \leq \boldsymbol{u}^{(phase)} \leq \boldsymbol{u}_{max}^{(phase)} \tag{14}$$

The optimizer consequently searches the optimal solution $\boldsymbol{x}, \boldsymbol{u}$ within these constraints. Specific values for $\boldsymbol{x}_{min}^{(phase)}$, $\boldsymbol{x}_{max}^{(phase)}$, $\boldsymbol{u}_{min}^{(phase)}$ and $\boldsymbol{u}_{max}^{(phase)}$ are presented and discussed in section V-A.

**Conditions for initial and final states**

Initial and final values of the state variables are defined as initial and final constraints. The optimizer searches the control

inputs $\boldsymbol{u}$ that optimally transfers the state vector $\boldsymbol{x}$ from the initial to the final states.

$$\boldsymbol{x}\left(t_0^{(c)}\right) = \boldsymbol{x}_0 \tag{15}$$

$$\boldsymbol{x}\left(t_f^{(d)}\right) = \boldsymbol{x}_f \tag{16}$$

It is important to note that optimal control allows to leave the final condition "free" for some of the variables. For example, it is unrealistic to require $m_t$ to have a certain exact value at FAF and thus any value within the path constraint can be taken. Specific values for $\boldsymbol{x}_0$ and $\boldsymbol{x}_f$ are presented and discussed in section V-A.

**Phase link conditions**

In order to guarantee continuous connection between the cruise and descent phases, we need to have the following phase link conditions

$$\boldsymbol{x}\left(t_f^{(c)}\right) = \boldsymbol{x}\left(t_0^{(d)}\right) \tag{17}$$

where all the aircraft states at $t_f^{(c)} = t_0^{(d)}$ (at the ToD) are equal in both the phases.

To summarize the above discussion, the target optimal control problem can be described as:

Determine

| | |
|---|---|
| States | $\boldsymbol{x}^{(c)}(t) = \{s(t), m(t)\}$ |
| | $\boldsymbol{x}^{(d)}(t) = \{V(t), s(t), h(t), m(t)\}$ |
| Controls | $\boldsymbol{u}^{(d)}(t) = \{\gamma(t), \delta_{SB}(t)\}$ |
| Final times | $t_f^{(c)}, t_f^{(d)}$ |

to minimize

Objective functional (11)

under the constraints of

Aircraft's dynamics (3)-(6)
Path constraints (12)-(14)
Initial and final conditions (15) (16)
Phase link conditions (17).

The initial times $t_0^{(c)}, t_0^{(d)}$ are excluded from the optimization since the former was assumed to be zero in Section III-A and the latter is constrained by the path constraints (12). Another note is that the final time for the cruise phase $t_f^{(c)}$ is equivalent to the time at ToD.

## IV. Solution methodology of the problem

### A. Pseudo-spectral method

Generally speaking, optimal control problems rarely have closed-form (or analytic) solutions, except for few known special cases (e.g. linear quadratic optimal control) [26]. Numerical methods are thus usually required to solve them. Solution methodologies for optimal control are mainly divided into two categories: direct methods and indirect methods [27]. In the past, the indirect methods were widely researched on because of their high accuracy and the assurance that the solution satisfies the first-order optimality conditions [28]. However, several critical computational disadvantages were found in the indirect methods and as a result the researchers' attentions have shifted to direct methods [27]. Among several variations of the direct methods, we chose the Legendre-Gauss pseudo-spectral method (LGPM). It was proved that LGPM's (discretized) solution satisfies the optimality conditions, which eliminates one of the common disadvantages of the direct methods [29].

LGPM discretizes the continuous time, state and control variables into so called collocation points. The flight dynamics and the objective functional are approximated using the variables at the collocation points and the constraints are imposed on each of them. Through this discretization, the original continuous optimal control problem is transcribed into a Non-Linear Programming (NLP) problem. In this study, the resulting NLP problem is solved by the Sequential Least SQuare Programming (SLSQP) method implemented in SciPy. When the optimal solution for the NLP problem is obtained, the solution for the original continuous optimal control problem is approximated by polynomials that interpolate the discrete solution.

An important feature of LGPM is that the collocation points, which are specified by the roots of the Legendre polynomials, are not placed at the edges of each phase corresponding to $t_0^{(phase)}$ and $t_f^{(phase)}$ (LG points in Fig. 2-4 in [29]). In order to consider the initial and final conditions, we add the missing phase edges to the collocation points only for the state variables. These points are not a root of the Legendre polynomials (Chapter 3 in [29]). The set of the overall points (collocation points and the phase edges) are called *nodes*. If the state variables in a phase have $N^{(phase)}$ collocation points and 2 phase edges, they totally have $N^{(phase)} + 2$ nodes in a phase. On the other hand, the control variables in a phase only have $N^{(phase)}$ collocation points. In this study, we have 2 state and 0 control variables and 1 final time for the cruise phase, and 4 state and 2 control variables and 1 final time for the descent phase. Therefore, totally $\big(2(N^{(c)} + 2) + 0N^{(c)} + 1\big) + \big(4(N^{(d)} + 2) + 2N^{(d)} + 1\big)$, equaling to

$$2N^{(c)} + 6N^{(d)} + 14 \tag{18}$$

variables are eventually decided in NLP. The number of collocation points are determined by the iterative process described in section IV-C.

### B. Initial Guess

The pseudo-spectral method (or resulting NLP) requires an initial guess, from which the calculation is initiated. In general, a non-convex optimization reaches a local optimum, or in other word a feasible solution in the vicinity of the given initial guess that satisfy all the constraints. Inappropriate initial guess selection often makes the optimization process converge into a poor local optimum or even sometimes prevents the optimizer

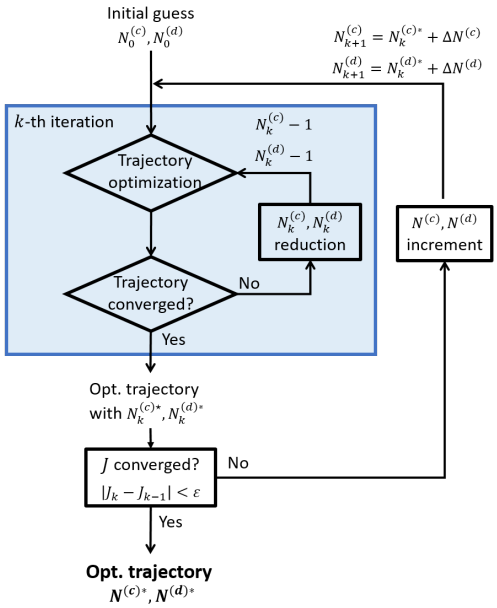


Fig. 1. Flow to determine the optimal number of collocation points.

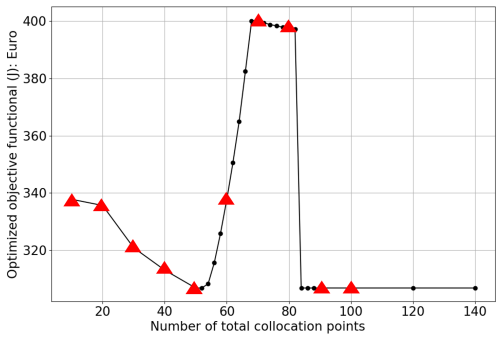


Fig. 2. Change of the objective functional $J_{opt}$ (for the reference ISA case) optimized with different number of collocation points. The red triangles show how $J_k$ changes in each iteration step in the proposed solution process.

from converging. An initial guess is to be chosen so that it satisfies all the equations of motion and the constraints. In this study, steady deceleration with steady path angle ($\gamma = -3°$in the geodetic coordinates system) is adopted in the descent phase, which is shown in Fig. 2.

### C. Iterative solution process

The numbers of collocation points $N^{(c)}, N^{(d)}$ (therefore the total number of considered collocation points $N^{(c)} + N^{(d)}$) have a strong impact on both calculation accuracy and time. In this study, an iterative algorithm is introduced to determine the optimal numbers $N^{(c)*}, N^{(d)*}$ as shown in Fig. 1. The collocation point location with respect to $t$ for each phase is automatically specified with a given $N^{(phase)}$, which corresponds to the roots of $N^{(phase)}$-th order of Legendre polynomials. The same number of collocation points are assumed in this study for both the cruise and descent phases ($N^{(c)} = N^{(d)}$) to simplify this solution process.

As shown in Fig. 1, the first iteration starts with a fairly small $N_0^{(phase)}$. Trajectory optimization is carried out, or in other words LGPM solves the optimal control problem, with the given numbers of collocation points. We set a patient limit for the iterative calculation ($\varepsilon_t^{patient} = 300$ s). If the optimization does not converge within the time limit, a new optimization starts. It goes with $N_1^{(phase)} - 1$ collocation points for each phase. The initial guess is also re-calculated with the new collocation points. When convergence is reached and the optimized trajectory is obtained (with tolerance for termination $f_{tol} = 10^{-6}$), the first iteration ends and the resulting $N_1^{(phase)}$ is expressed as $N_1^{(phase)*}$. The second iteration starts with $N_2^{(phase)} = N_1^{(phase)*} + \Delta N^{(phase)}$ collocation points. In this study, we set $\Delta N^{(c)} = \Delta N^{(d)} = 5$. If the absolute error of objective functional value gets smaller than a pre-set tolerance $\varepsilon = 1.54$ €, corresponding to the fuel price for 1 kg of fuel burn, the iterative algorithm is terminated and the optimal numbers of collocation points $N^{(c)*}, N^{(d)*}$ (therefore totally $N^{(c)*} + N^{(d)*}$) are finally determined.

The change of optimized objective functional $J_{opt}$ with $N_k^{(c)} + N_k^{(d)}$ in each iteration is shown in Fig. 2 (for the reference case discussed in the next section). In the reference case, calculations in every $k$-th iteration terminated within $\varepsilon_t^{patient}$ so the reduction $N_k^{(phase)}$ did not occur. We started the iterative process with $N_0^{(phase)} = 5$ and the process terminated with $N^{(phase)*} = 50$. Therefore, optimal number of collocation points was determined as $N^{(c)*} + N^{(d)*} = 100$. In the graph, some more results, represented with black dots, are also depicted to show the overall shape of $J$. The plot shows that a large transition happens when $68 \leq N \leq 82$. This jump is caused because the optimizer converged to a local minimum different from the finally obtained optimal trajectory, which can be seen also in Fig. 3 (case 70). We believe the above determined number of collocation points is reasonable as the change of $J$ stays within a range of $\varepsilon$ even with more collocation points up to 140 total collocation points (see Figs. 2 and 3). With the optimized number of collocation points, the following NLP problem totally has 414 decision variables according to (18).

One can understand from Fig. 2 that the iterative algorithm terminates with a different number of points if different adjustment method $\Delta N^{(phase)}$ is applied. When $\Delta N^{(phase)} = 2$ for example, it finishes the process with 72 points and convergence is judged to the other local optimum around 400 €, giving us an inadequate result. The output of the iterative process was therefore confirmed by testing with different initial guess or by applying more strict value of $\varepsilon$.

Fig. 3 shows how the optimized airspeed and altitude time histories converge with an increasing number of collocation points starting from the initial guess. The blue thick line shows the initial guess. The trajectories corresponding to 90 and 100 collocation points are overlapped since they are converged.

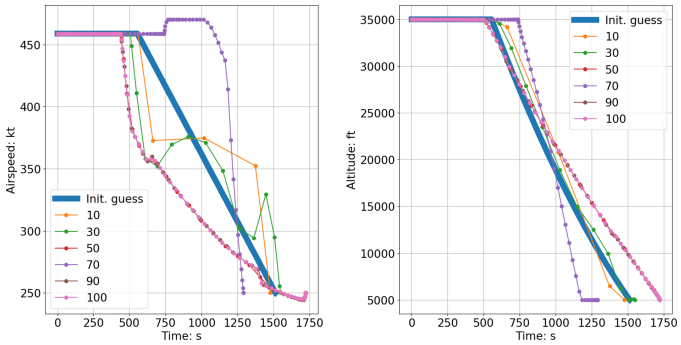


Fig. 3. Trajectories optimized with different number of collocation points in the proposed reference case. They show how the trajectory converges from the initial guess to the finally optimized solution as the number of collocation points increases.

## V. Numerical Simulation

### A. Scenario

The study considers Airbus A320, whose total mass is 63700 kg, flying at cruise altitude (35000 ft) with a cruise airspeed (460 kt equivalent to Mach number 0.8 in the ISA conditions). The aircraft is going to descend down to the FAF located 165 NM away from the initial position (along-track distance) and at 5000 ft above the ground. With this distance to the FAF, the trajectory has both cruise and descent phases. The fuel cost $C_f$ is assumed to be 0.61 €/kg. The parameter values were obtained from BADA4 [25] except for what is mentioned below.

**Objective functional**

In this case study, we focus on the minimum fuel CDO, thus $C_I = 0$ in (11), and therefore only fuel burn is considered in the objective functional.

**Initial and final states**

Initial and final conditions for the state variables are specified in Table I. The initial conditions for $V, h, m$ come from the assumed scenario described above. As discussed in Section III-A, $s$ is initialized at the initial point. The final conditions for $s$ and $h$ are determined by the FAF location defined above. Final condition is not imposed on $m$ and thus it is allowed to have any value within its path constraints.

**Path constraints**

Specific values for the minimum and maximum path constraints, listed in Table I, define the area of interest in which the optimal variable histories are searched. Note that constraints for $V, h, \gamma$ are imposed only in the descent phase, since they are excluded from the optimization for the cruise phase (see Section III-B). The maximum airspeed is determined by Mach number 0.82 at the initial altitude, whereas the minimum corresponds to the stall speed. Constraints for $s$ and $h$ mean altitudes above the cruise altitude and below the FAF altitude are not allowed.

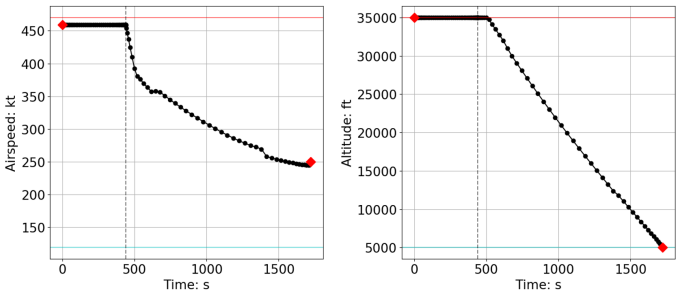


Fig. 4. $V$ and $h$ time histories (reference ISA case).

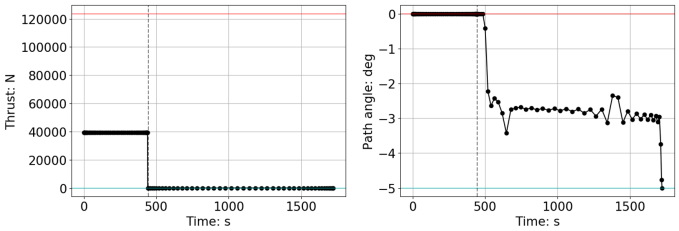


Fig. 5. $F_T$ and $\gamma$ time histories (reference ISA case).

For the control variables, maximum thrust of A320 is obtained from the aircraft performance model COALA, which the Institute of Aviation and Logistics at TU Dresden has been developing [30]. The altitude effect on the maximum thrust is neglected for simplification. Zero thrust is assumed for minimum (idle) thrust and the BADA4 fuel consumption models correctly consider remaining fuel flow also in that context. As for the descent angle, the maximum is $\gamma = 0.0$ °, which means that horizontal flight segments are also allowed during descent, thus reflecting typical current CDO operational operations and in-line with [1]. The minimum path angle $\gamma = -5.0$ °covers typical descent angle (about -3.0 °) and also allows expedite descent if required.

TABLE I
Initial and Final Conditions and Path Constraints

| Variable | | Init | Fin | Min | Max |
|---|---|---|---|---|---|
| $V$ | [kt] | 460 | 250 | 119 | 472.6 |
| $s$ | [NM] | 0 | 165 | 0 | 500 |
| $h$ | [ft] | 35000 | 5000 | 5000 | 35000 |
| $m$ | [kg] | 63700 | Free | 54200 | 63700 |
| $F_T$ | [N] | - | - | 0 | 123440 |
| $\gamma$ | [°] | - | - | -5.0 | 0.0 |
| $\delta_{SB}$ | [-] | - | - | 0 | 1 |

### B. Simulation Results - reference scenario

First, trajectory calculated under ISA condition is presented as a reference to discuss fundamental features of the optimization described in this paper. Time histories of $V$ and $h$ are shown in Fig. 4 and of $F_T$ and $\gamma$ in Fig. 5 with black dots representing the collocation points. The red and blue horizontal lines show the minimum and maximum path constraints, and the red diamonds in Fig. 4 indicate the initial and final conditions. The graphs clearly shows the solution

was found within the path constraints and satisfies the initial and final conditions. The gray vertical dashed lines indicate where the phase transition from cruise to descent occurred. The optimized trajectory for this case does not use speed brake.

In this study, the aircraft is regarded as going into descent phase when $\gamma < -0.1°$for the first time and the corresponding collocation point location is seen as ToD location. From the $h$ plot in Fig. 4, one can understand that the phase transition (gray vertical dashed line) does not match the ToD location. Early in the descent phase $(440 \text{ s} \leq t \leq 490 \text{ s})$, the aircraft decelerates with idle thrust while keeping the cruise altitude. The similar speed trend can also be found in [19]. This deceleration in cruise comes because the optimal descent speed at the cruise altitude has a gap from the given cruise speed and thus the optimizer tried to reduce it while keeping the cruise altitude. The considered flight dynamics allows such flight as the simplified cruise dynamics is a subset of the descent dynamics except for the thrust settings (section III-B). Therefore the flight being possible in the cruise is also possible in the descent as long as it is feasible while idle thrust is applied. ToD is located at $t = 484$ s. The fuel costs $J$ finally become 307 € equivalent to 501 kg fuel burn. The final time $t_f$ is 1723 s. The airspeed curve in Fig. 4 has a bound or a phase transition during descent (from around 620 s to 1400 s). This can be explained by the observation that idle and general fuel consumption models in BADA4 $FC = \max(FC_{idle}, FC_{gen})$ swap. This study adopts the two models but the bounds disappears if only one of them is used.

### C. Simulation results - Wind variation

A given wind prediction is assumed to have uncertainties around the reference scenario, which is up to 50 kt of both horizontal head and tail wind. The wind speed variation is assumed to be fixed in the entire descent. Figs. 6 and 7 show changes of CDO trajectory and the corresponding fuel burn respectively with the expected wind variation.

Fig. 6 shows stronger head wind causes longer cruise (therefore later ToD location) and steeper descent path angle, whereas stronger tail wind leads to shorter cruise (earlier ToD) and shallower descent. The resulting ToD location is shifted 18 s or 17.5 NM before and 208 s or 16.9 NM after the reference at most. As for the fuel costs $J$, stronger head wind requires more fuel per ground distance and stronger tail wind requires less (Fig. 7), ranging from -117 kg to +140 kg compared to the reference. This variance can be explained mostly by different lengths of the cruise phase with regard to the ground.

Expected solution space is defined as the area consisting of the varied trajectories in the Figs. 6 and 7. If uncertainty range related to wind is somehow quantified to range from 50 kt head to 50 kt tail wind, we can show pilots how the uncertainty changes their CDO trajectory and fuel burn using the solution space. The edge of it presents trajectories in extreme cases where 50 kt head or tail wind blows all the time. Pilots can expect that they will actually fly somewhere in this space.

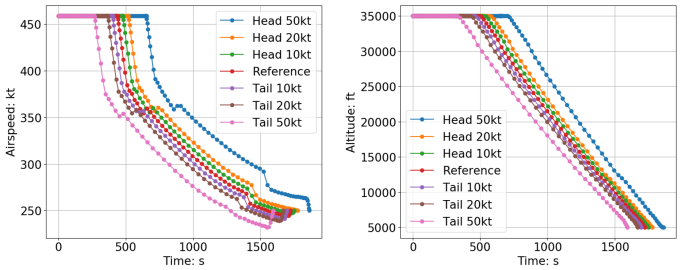


Fig. 6. Change of $V$ and $h$ time histories with wind variation.

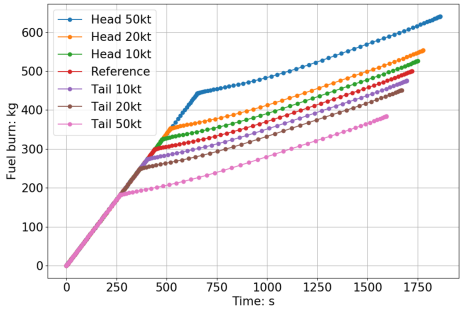


Fig. 7. Change of fuel burn time history with wind variation.

Deviation from this solution space motivates them to conduct additional path planning or trajectory re-optimization.

### D. Simulation results - Temperature variation

Temperature prediction uncertainty by 10 K higher and lower than ISA is assumed in this study, and change of other atmospheric variables such as air density and pressure due to the temperature change is ignored.

Fig 8 shows not as large difference in $V$ and $h$ with the temperature variation as seen in the windy cases. Lower temperature caused later ToD. In the lowest temperature case (-10 K), ToD is located 8.0 s or 0.9 NM later than that for the reference case whereas 4.0 s or 0.4 NM later in the highest temperature (+10 K) case. On the other hand, fuel burn has clearer difference (Fig. 9). According to the figure, the aircraft needs more fuel in a lower temperature case, ranging from -8.8 kg (+10K case) to +25.4 kg (-10 K case) compared to the reference ISA case. This is because larger required thrust is necessary to balance with larger drag caused by lower temperature. It increases the Mach number $M = V/\sqrt{\kappa RT}$ with the assumed constant cruise airspeed (see Section III), as shown in Fig. 10. As the $C_D$ model in BADA4 has polynomial forms and each term contains $1 - M^2$ to an integer power in denominators. Therefore, the increased Mach number results in higher drag coefficient and the higher balanced cruise thrust (Fig. 10), which leads to more fuel burn.

Figs. 6 and 8 show that pilots need to expect a smaller solution space with temperature variation than with the wind variation.

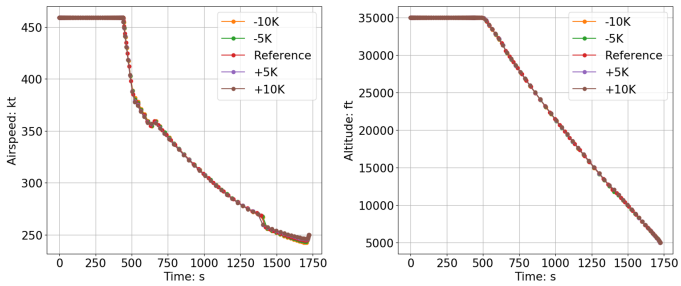


Fig. 8. Change of $V$ and $h$ time histories with temperature variation.

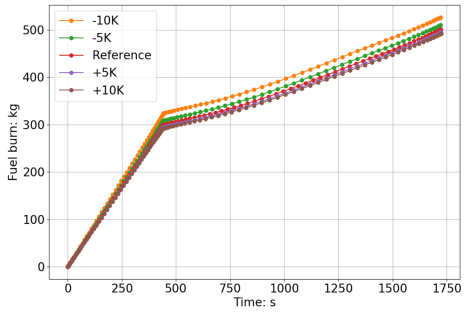


Fig. 9. Change of fuel burn time history with temperature variation.

## VI. Conclusion and Future Works

This study established a way of designing and evaluating a CDO solution space with given types of prediction uncertainties. The solution space consisted of optimized CDO trajectories corresponding to varied prediction errors. The trajectory optimization problem was formalized as a multi-phase optimal control problem and solved with the Legendre-Gauss pseudo-spectral method (LGPM). The trajectory was optimized through iterative solution process, which determines the optimal number of collocation points.

Numerical results showed that the wind speed variation up to 50 kt had larger expected solution space than the temperature deviation up to 10 K. The maximum head wind caused approximately 208 s or16.9 NM later ToD and the maximum head wind caused 17.5 NM or 17.9 s earlier ToD, requiring +140 kg and -117 kg fuel burn to the reference case. As for the temperature deviation, 8.0 s or 0.9 NM at most later ToD was calculated in the lowest temperature case. Early ToD was not obtained. Even though the ToD location did not have significant difference, the temperature variations certainly affected the amount of fuel burn, ranging from -8.8 kg (+10 K case) to +25.4 kg (-10 K case) to the reference.

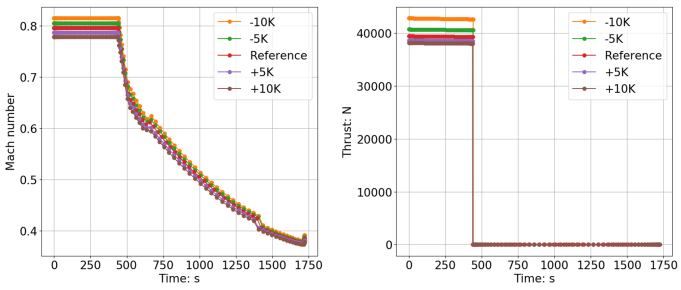


Fig. 10. Change of Mach number and $F_T$ time histories with temperature variation.

If uncertainty range is somehow quantified, we can show pilots and ATCOs how uncertainties change the CDO trajectory and fuel burn using the proposed solution space. Deviation from this solution space motivates them to conduct additional path planning or trajectory re-optimization. We believe these designed solution spaces and quantified ToD locations can support them by giving them a good reference when they robustly plan and execute continuous descent operations and thus also can improve the throughput on runways.

The next step of this research would be to design a metrics to determine the second best solution located in the solution space. For this purpose, change of the objective functional $J$ depending on the change of the discretized NLP decision variables (Jacobian) will be investigated. Aspects of time will be introduced, such as required time of arrival in the final conditions and different $C_I$ in the objective functional to consider time costs. After designing the metrics, the deterministic problem setting will be expended to stochastic by introducing uncertainties modeled with probability density functions. In terms of improving the numerical computation, selection of an initial guess with good quality will be further investigated to avoid stacking a bad local optimum. From a more practical viewpoint, study on multiple aircraft (at least two successive aircraft) would be an interesting application of the proposed method to analyze how uncertainties propagate in the traffic flow.

## Acknowledgment

This work is a part of a project *Optimized CDO under Uncertain Environmental and Mission Conditions* (project number: 327114631) financed by German Research Foundation (DFG).

## References

[1] *Continuous descent operations (CDO) manual*, Doc 9931 ed., International Civil Aviation Organization, 2010.

[2] "European ATM master plan progress report 2019," SESAR, 2019.

[3] H. Fricke, C. Seiß, and R. Herrmann, "Fuel and energy benchmark analysis of continuous descent operations," in *11th USA/Europe Air Traffic Management Research and Development Seminar (ATM Seminar 2015)*, 2015.

[4] S. G. Park and J. P. Clarke, "Vertical trajectory optimization for continuous descent arrival procedure," in *AIAA Guidance, Navigation, and Control (GNC) Conference*, 2012.

[5] P. M. A. De Jong, "Continuous descent operations using energy principles," Ph.D. dissertation, Delft University of Technology, 2014.

[6] L. Stell, "Prediction of top of descent location for idle-thrust descents," in *Ninth USA/Europe Air Traffic Management Research and Development Seminar (ATM Seminar 2011)*, 2011.

[7] J. Rosenow and M. Schultz, "4D trajectory prediction with stochastic input parameters," in *Advanced Aircraft Efficiency in a Global Air Transport System*, 2018.

[8] D. González-Arribas, M. Soler, and M. Sanjurjo-Rivo, "Robust aircraft trajectory planning under wind uncertainty using optimal control," *Journal of Guidance, Control, and Dynamics*, vol. 41, no. 3, pp. 673–688, 2018.

[9] R. Dalmau and X. Prats, "How much fuel and time can be saved in a perfect flight trajectory?" in *2014 International Conference on Research in Air Transportation (ICRAT2014)*, 2014.

[10] I. Wilson and F. Hafner, "Benefit assessment of using continuous descent approaches at Atlanta 3D precision Approaches," in *Digital Avionics Systems Conference (DASC)*, 2005, pp. 1–7.

[11] L. Jin, Y. Cao, and D. Sun, "Investigation of potential fuel savings due to continuous-descent approach," *Journal of Aircraft*, vol. 50, no. 3, pp. 807–816, 2013.

[12] M. Y. Pereda Albarrán, A. K. Sahai, and E. Stumpf, "Aircraft noise sound quality evaluation of continuous descent approaches," in *International Congress amd Exposition on Noise Control Engineering (INTER-NOISE 2017)*, aug 2017.

[13] T. Thompson, B. Miller, C. Murphy, and S. Souihi, "Environmental impacts of continuous-descent operations in Paris and New York regions," in *Tenth USA/Europe Air Traffic Management Research and Development Seminar (ATM Seminar 2013)*, 2013.

[14] J. Ellerbroek, M. Inaad, and J. Hoekstra, "Fuel and emission benefits for continuous descent approaches at Schiphol," in *2018 International Conference on Research in Air Transportation (ICRAT2018)*, 2018.

[15] J. P. Clarke, N. Ho, L. Ren, J. Brown, K. Elmer, K. O. Tong, and J. Wat, "Continuous descent approach: design and flight test for Louisville international airport," *Journal of Aircraft*, vol. 41, no. 5, pp. 1054–1066, 2004.

[16] M. Kaiser, M. Schultz, and H. Fricke, "Automated 4D descent path optimization using the enhanced trajectory prediction model (ETPM)," in *5th International Conference on Research in Air Transportation (ICRAT2012)*, 2012, pp. 1–8.

[17] S. G. Park and J. P. Clarke, "Optimal control based vertical trajectory determination for continuous descent arrival procedure," *Journal of Aircraft*, vol. 52, no. 5, pp. 1–12, 2015.

[18] R. Dalmau, R. Verhoeven, N. De Gelder, and X. Prats, "Performance comparison between TEMO and a typical FMS in presence of CTA and wind uncertainties," in *2016 IEEE/AIA 36th Digital Avionics Systems Conference (DASC)*, sep 2016.

[19] M. Soler, "Commercial aircraft trajectory planning based on multiple mixed-integer optimal control," Ph.D. dissertation, Universidad Rey Juan Carlos, 2013.

[20] E. Casado, C. Goodchild, and M. Vilaplana, "Identification and initial characterization of sources of uncertainty affecting the performance of future trajectory management automation systems," in *2nd International Conference on Application and Theory of Automation in Command and Control Systems (ATACCS'2012)*, 2012, pp. 170–175.

[21] S. Mondoloni, "Aircraft Trajectory Prediction Errors: Including a Summary of Error Sources and Data (Version 0.2) FAA/Eurocontrol Action Plan 16 Common Trajectory Prediction Capabilities," FAA/Eurocontrol, Tech. Rep., 2006.

[22] P. M. A. De Jong, N. De Gelder, R. Verhoeven, F. Bussink, R. Kohrs, M. Van Paassen, and M. Mulder, "Time and energy management during descent and approach: batch simulation study," *Journal of Aircraft*, vol. 52, no. 1, pp. 190–203, 2015.

[23] R. Verhoeven, R. Dalmau, X. Prats, and N. De Gelder, "Real-time aircraft continuous descent trajectory optimization with ATC time constraints using direct collocation methods," *29th Congress of the International Council of the Aeronautical Sciences, ICAS 2014*, pp. 1–9, 2014.

[24] L. Evans, "An introduction to mathematical optimal control theory."

[25] A. Nuic and V. Mouillet, "User manual for the base of aircraft data (BADA) family 4," EUROCONTROL, Tech. Rep. 12/11/22-58, Version 1.3, 2016.

[26] E. Todorov, "Optimal Control Theory," in *Bayesian Brain*. The MIT Press, 2006.

[27] G. Q. Huang, Y. P. Lu, and Y. Nan, "A survey of numerical algorithms for trajectory optimization of flight vehicles," *Science China Technological Sciences*, vol. 55, no. 9, pp. 2538–2560, sep 2012.

[28] D. Benson, G. Huntington, T. Thorvaldsen, and A. Rao, "Direct trajectory optimization and costate estimation via an orthogonal collocation method," *Journal of Guidance, Control and Dynamics: Engineering Notes*, vol. 29, no. 6, pp. 1435–1440, 2006.

[29] G. Huntington, "Advancement and abalysis of a Gauss pseudospectral transcription for optimal control problems," Ph.D. dissertation, Massachusetts Institute of Technology, 2007.

[30] S. Förster, J. Rosenow, M. Lindner, and H. Fricke, "A toolchain for optimizing trajectories under real weather conditions and realistic flight performance," in *Greener Aviation 2016*, 2016.